Parathyroid Imaging: The Importance of Dual-Radiopharmaceutical Simultaneous Acquisition with ^{99m}Tc-Sestamibi and ^{123}I

Scott A. Caveny[1], William C. Klingensmith III[1], Wesley E. Martin[1], Adrienne Sage-El[1], Robert C. McIntyre, Jr.[2], Christopher Raeburn[2], and Pamela Wolfe[3]

[1]Division of Nuclear Medicine, Department of Radiology, University of Colorado School of Medicine, Aurora, Colorado; [2]Division of GI, Tumor and Endocrine Surgery, Department of Surgery, University of Colorado School of Medicine, Aurora, Colorado; and [3]Department of Biostatistics and Informatics, Colorado School of Public Health, Aurora, Colorado

Our objective was to compare the accuracy of 3 imaging protocols for the detection of parathyroid adenomas: single-tracer, dual-phase imaging with ^{99m}Tc-sestamibi; dual-tracer, single-phase imaging with simultaneous acquisition of ^{99m}Tc-sestamibi and ^{123}I images; and dual-tracer, dual-phase imaging with simultaneous acquisition of ^{99m}Tc-sestamibi and ^{123}I images. **Materials:** Thirty-seven patients with surgical proof of parathyroid adenomas were evaluated. Three different protocols were derived from a single study in each patient, resulting in an intrapatient intrastudy comparison. The first derived protocol was the conventional dual-phase protocol with ^{99m}Tc-sestamibi consisting of anterior and anterior-oblique pinhole images of the neck at 15 min and 3 h plus parallel-hole images of the neck and upper chest at both imaging times. The second derived protocol was a dual-tracer, single-phase protocol consisting of administration of ^{123}I followed 2 h later by ^{99m}Tc-sestamibi. Fifteen minutes later, anterior and anterior oblique pinhole images of the ^{99m}Tc-sestamibi and ^{123}I were acquired simultaneously, allowing generation of perfectly coregistered subtraction images. Parallel-hole images of the neck and upper chest were also obtained. The third protocol was the same as the second except that the same imaging protocol was repeated at 3 h. Two experienced nuclear medicine physicians indicated the location of any identified lesion and graded the certainty of diagnosis on a 3-point scale. **Results:** Thirty-seven patients had 41 parathyroid adenomas. For the 2 observers combined, the localization success rate was 66% for the single-tracer, dual-phase protocol; 94% for the dual-tracer, single-phase protocol; and 90% for the dual-phase, dual-tracer protocol. Both dual-tracer protocols were significantly more accurate than the single-tracer protocol ($P < 0.01$); there was no significant difference between the 2 dual-tracer protocols. In addition, the degree of certainty of localization was greater with the 2 dual-tracer protocols than the single-tracer protocol ($P < 0.001$). **Conclusion:** A dual-tracer, single-phase parathyroid imaging protocol consisting of simultaneous acquisition of ^{99m}Tc-sestamibi and ^{123}I images with pinhole collimation at 15 min and perfectly coregistered subtraction results in a higher degree of accuracy and a greater degree of diagnostic certainty than the commonly used single-tracer, dual-phase protocol of imaging ^{99m}Tc-sestamibi alone at 15 min and 3 h. The addition of delayed imaging to the dual-tracer protocol did not improve results.

Key Words: parathyroid imaging; ^{99m}Tc-sestamibi; ^{123}I; simultaneous acquisition; subtraction

Primary hyperparathyroidism is the most common cause of hypercalcemia in otherwise healthy adults (*1*). Historically, surgical excision of parathyroid adenomas required bilateral exploration of the neck (*2*). With the advent of preoperative imaging, intraoperative parathormone assay, and hand-held γ-detectors, a minimally invasive approach is now commonly used, which results in better cosmesis, a lower risk of temporary hypocalcemia, and the ability to perform a parathyroidectomy on some patients on an outpatient basis. Because of the success of minimally invasive surgery, there is a significant need to optimize preoperative parathyroid imaging studies (*3–6*).

Several different parathyroid imaging protocols have been reported. They vary in whether pinhole or parallel-hole collimation is used; whether SPECT with or without CT is used; whether 1 or 2 tracers are used; and, if 2 tracers are used, whether there is simultaneous acquisition, which allows perfectly coregistered subtraction of the thyroid gland from the thyroid gland plus any parathyroid adenoma (*7–12*). The simplest and probably most widely used protocol is the single-tracer, dual-phase study with ^{99m}Tc-sestamibi, which was first reported by Coakley et al. in 1989 and rapidly became the standard of care because of its favorable results and relative simplicity (*13–17*).

However, the single-tracer, dual-phase method with ^{99m}Tc-sestamibi depends on washout of the ^{99m}Tc-sestamibi from the thyroid over time but not from any parathyroid adenoma.

This pattern occurs in about 70%–75% of patients. In the remainder of patients, ^{99m}Tc-sestamibi washes out of the parathyroid adenoma as fast as it washes out of the thyroid (*18,19*). Thus, a parathyroid adenoma that blends into the thyroid at 15 min and washes out at the same rate as thyroid is likely to go undetected. In a review article in 2004, Mullan reported significant success in identifying these problematic parathyroid adenomas by performing simultaneous acquisition of the ^{99m}Tc-sestamibi and ^{123}I images at 15 min (*3*). The simultaneous acquisition allows perfectly coregistered subtraction, which is required to confidently interpret small areas of activity that remain after subtraction of the ^{123}I thyroid image from the ^{99m}Tc-sestamibi image of thyroid plus parathyroid adenoma. They also performed simultaneous acquisition imaging at 3 h. Although the dual-tracer simultaneous acquisition approach has been periodically published for some time, most institutions continue to use the single-tracer, dual-phase protocol with ^{99m}Tc-sestamibi (*20–24*)

We sought to determine the increase in accuracy in identifying the location of parathyroid adenomas with the dual-tracer simultaneous-acquisition method compared with the single-tracer, dual-phase protocol, both with pinhole collimation. We also evaluated the incremental value of acquiring delayed 3-h images in the dual-tracer approach in addition to the 15-min images. The images for all 3 protocols were obtained from a single study in each patient so that the comparisons were performed on an intrapatient and intrastudy basis.

MATERIALS AND METHODS

Patient Accrual

Forty consecutive patients who underwent dual-radiopharmaceutical dual-phase parathyroid imaging and surgery for primary hyperparathyroidism in a 10-mo period were included. All patients had blood calcium and serum parathormone determinations before referral for nuclear medicine parathyroid imaging. The study was approved by the Institutional Review Board.

Imaging Protocol

Patients were initially given 22.2 MBq (600 μCi) of ^{123}I orally. Two hours later, the patients were given 925 MBq (25 mCi) of ^{99m}Tc-sestamibi intravenously. Dual-phase imaging was performed at 15 min and at 3 h after administration of the ^{99m}Tc-sestamibi. The images were acquired with an E.CAM γ-camera with an energy resolution of 9% (Siemens Medical Solutions). At each time, 5-min pinhole images of the neck in the anterior and both anterior oblique projections (45°) were obtained with a 4-mm pinhole insert. In addition, at both times a 5-min low-energy high-resolution parallel-hole collimator image with a field of view extending from the submandibular glands to the left ventricle in the anterior projection was obtained.

The ^{99m}Tc-sestamibi and ^{123}I images were acquired simultaneously with a 12% energy window centered at 140 keV for ^{99m}Tc-sestamibi and an 8% symmetric energy window centered at 159 keV for ^{123}I (*3*). There was no correction for cross talk (*3*). Subtraction images were constructed for all pairs of ^{99m}Tc-sestamibi and ^{123}I pinhole images. The subtractions were done manually by increasing the amount of subtraction of the ^{123}I thyroid image from the ^{99m}Tc-sestamibi image until the thyroid was essentially no longer visible. The thyroid bed in the subtracted image had a salt-and-pepper appearance because of differences in statistical mottling between the initial ^{99m}Tc-sestamibi

and ^{123}I images. Quantitative algorithms were less reliable in achieving the appropriate amount of subtraction of the thyroid.

The images from each patient study were used to create 3 different protocols. The first protocol was a single-tracer (^{99m}Tc-sestamibi only), dual-phase study with pinhole and parallel-hole images at 15 min and 3 h. The second protocol was a dual-tracer (^{99m}Tc-sestamibi and ^{123}I), single-phase study with pinhole and parallel-hole images at 15 min only. And the third protocol was a dual-tracer, double-phase study with pinhole and parallel-hole images at 15 min and 3 h.

The effective whole-body dose from 22.2 MBq of ^{123}I is 4.2 mSv (0.42 rem), and from 925 MBq of ^{99m}Tc-sestamibi the effective whole-body dose is 8.4 mSv (0.84 rem), for a combined effective dose of 1.26 rem (*25*). This is well within the range of other diagnostic studies that use ionizing radiation.

Image Interpretation

Each of 2 experienced nuclear medicine physicians independently interpreted the 3 protocols that were derived from each study in order of increasing complexity. The single-tracer, dual-phase protocol was interpreted first for all patients. Then, the dual-tracer, single-phase protocol was interpreted for all patients. Finally, the dual-tracer, dual-phase protocol was interpreted for all patients. The readers were unaware of the identity of the patient, and the sequence of studies within each interpretation session was randomized. There was at least 1 wk between interpretations of the 3 protocols for each interpreting physician. Examples of the 3 protocols derived from a single study in 1 patient are shown in Figures 1–3.

Each protocol for each study was interpreted on a 4-point scale, with zero indicating no evidence of a parathyroid adenoma and 1 through 3 indicating a focus of activity with increasing contrast with the surrounding activity. One indicated a possible parathyroid adenoma, 2 a probable parathyroid adenoma, and 3 a definite parathyroid adenoma. In addition to the certainty of a parathyroid adenoma, the interpreting physician indicated the location of the abnormality with respect to side (right or left) and with respect to the thyroid lobes (superior, mid, or inferior, as well as posterior, in the same plane as, or anterior to the thyroid). The anatomic location of ectopic parathyroid tissue that was above or below the thyroid was described. If a study showed more than 1 parathyroid abnormality, the interpretation process was repeated for each abnormality, beginning with the most obvious abnormality.

Surgery

All operations were performed by 1 of 2 endocrine surgeons, 2 otolaryngologic surgeons, and 1 thoracic surgeon. The surgical finding, including intraoperative parathormone values and the histopathologic findings, was used as diagnostic proof.

Operations included minimally invasive parathyroidectomy, unilateral exploration, bilateral exploration, hemithyroidectomy, and near-total thyroidectomy as indicated. Intraoperative assays of serum parathormone were done at the beginning of surgery and after the removal of each parathyroid gland. An intraoperative decrease in blood parathormone level of at least 50% was considered evidence of curative surgery. Histologic analysis was conducted on specimens, and intraoperative histologic analysis by frozen section was done as indicated. Occasionally, an intraoperative γ-probe was used.

Statistical Analysis

Accuracy, the primary outcome, was defined as the proportion of locations that were correctly identified. The site location was coded

FIGURE 1. Example of single-tracer, dual-phase protocol. Pinhole images of neck were obtained in anterior (ANT), right anterior oblique (RAO), and left anterior oblique (LAO) projections at 15 min and 3 h after intravenous injection of ^{99m}Tc-sestamibi. In addition, parallel-hole collimator image from submandibular salivary glands to left ventricle was obtained in anterior projection at 15 min and 3 h (not shown). There is subtle suggestion of adenoma at upper pole of left lobe of thyroid at both 15 min and 3 h. ^{99m}Tc-sestamibi washes out of parathyroid adenoma in a manner similar to the way it washes out of thyroid.
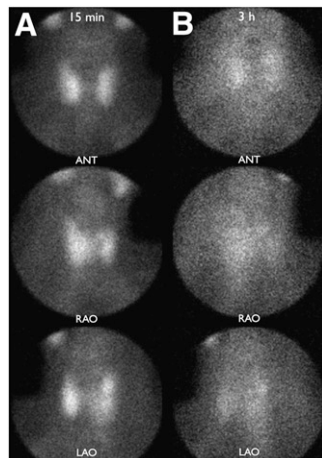
as correct if the reader's response matched the surgical result exactly or within half the distance between the inferior and superior poles to allow for variation in the accuracy of the surgical description. Thus, an imaging location of mid thyroid was considered to match a surgical location of superior or inferior and vice versa.

The accuracy for the 3 protocols was compared statistically using a pseudo likelihood estimate for the differences between protocols (single-tracer, dual-phase, vs. dual-tracer, single-phase, or single-tracer, dual-phase, vs. dual-tracer, dual-phase) in a repeated-measures model for the binary outcome (26). Reader and protocol were entered as main effects; patient was designated as a repeated effect. A similar model was used to evaluate the certainty score recoded from 0, 1, 2, or 3 to a binary variable coded 1 if score was 3 and 0 if the score was other than 3. Descriptive statistics for the number of lesions located, the accuracy rate, and its 95% exact binomial confidence interval were also computed. Associations among gland size (log-transformed to stabilize the variance), parathormone level, and calcium level were estimated with the Pearson product-moment correlation coefficient.

RESULTS

Patient Data

A total of 40 patients underwent nuclear medicine parathyroid imaging and operation for removal of abnormal parathyroid tissue. In 1 patient, no abnormal parathyroid tissue was identified, and this patient was excluded from analysis. In 2 patients, abnormal parathyroid tissue was found in lymph nodes consistent with parathyroid cancer. In both patients, the nodal cancer was identified in the parathyroid imaging study, but these 2 patients are not considered further. No patient had parathyroid hyperplasia.

The remaining 37 patients had 1 or more parathyroid adenomas. There were 28 women and 13 men. The average age for women was 56.8 y (range, 36–77 y), and for men it was 57.7 y (range, 34–81 y). Six of the 37 patients had had a previous parathyroidectomy or partial thyroidectomy. Three patients were taking replacement thyroxine at the time of imaging.

For all 37 patients with 1 or more adenomas, the average blood calcium level was 10.8 mg/dL (range, 9.6–12.3 mg/dL)

and the average serum parathormone level at the time of surgery was 131.4 pg/mL (range, 51–259 pg/mL). Excluding 3 patients with multiple parathyroid adenomas, there was a significant correlation between the serum parathormone level and the blood calcium level ($r = 0.35$; $P = 0.042$).

Surgical Results

Thirty-four patients had 1 parathyroid adenoma, 2 patients had 2 adenomas, and 1 patient had 3 adenomas, for a total of 41 adenomas. Of the 37 patients with parathyroid adenomas, 33 had 1 or more adenomas in the region of the thyroid. Of these 33 patients, 16 underwent minimally invasive surgery, 7 underwent unilateral neck exploration (including 1 patient with an intrathyroidal parathyroid adenoma), 3 underwent bilateral neck exploration, 4 had a hemithyroidectomy (including 2 additional patients with intrathyroidal parathyroid adenomas), and 3 had a subtotal thyroidectomy. Four patients had ectopic parathyroid adenomas some distance from the thyroid. Of these 4 patients, 1 had an adenoma in the mid mediastinum, 2 had adenomas in the superior thymus, and 1 had an adenoma at the left carotid bifurcation. The ectopic adenomas in the region of the left carotid bifurcation and superior thymus were seen within the field of view of the pinhole images and also in the larger field of view of the parallel-hole collimator images. The adenoma in the mid mediastinum was seen only in the parallel-hole collimator image.

The average initial intraoperative parathormone level was 131.4 pg/mL (range, 51–259 pg/mL), and the average final post-resection intraoperative parathormone level was 29.8 pg/mL (range, 8–59 pg/mL). The average percentage decrease in the intraoperative parathormone level from before resection to after resection was 76.1% (range, 38%–95%).

Pathologic Findings

The histologic diagnosis of an adenoma was based primarily on the presence of cellular hyperplasia. The average weight of the adenomas was 672 mg (range, 60–4,130 mg). Excluding the 3 patients with multiple parathyroid adenomas, there was a significant correlation between the parathormone level and the size of the parathyroid adenomas ($r = 0.50$; $P = 0.003$).

Protocol Analysis

The interpretation results on a per-adenoma basis are shown in Table 1. The single-tracer, dual-phase ^{99m}Tc-sestamibi protocol detected fewer adenomas and with a lower degree of certainty, that is, fewer grade 3 (definite adenoma) interpretations, than either of the dual-tracer ^{99m}Tc-sestamibi and ^{123}I protocols ($P < 0.001$). There was little difference between the 2 dual-tracer protocols in any grade. There were 2 mislocalizations, both of which occurred in the single-tracer, dual-phase protocol. The results, with the 3 positive grades combined and averaged for the 2 readers, are summarized graphically in Figure 4.

In patients with multiple adenomas, the nonprimary, less obvious adenomas accounted for a disproportionate number of undetected adenomas. For the single-tracer protocol, reader
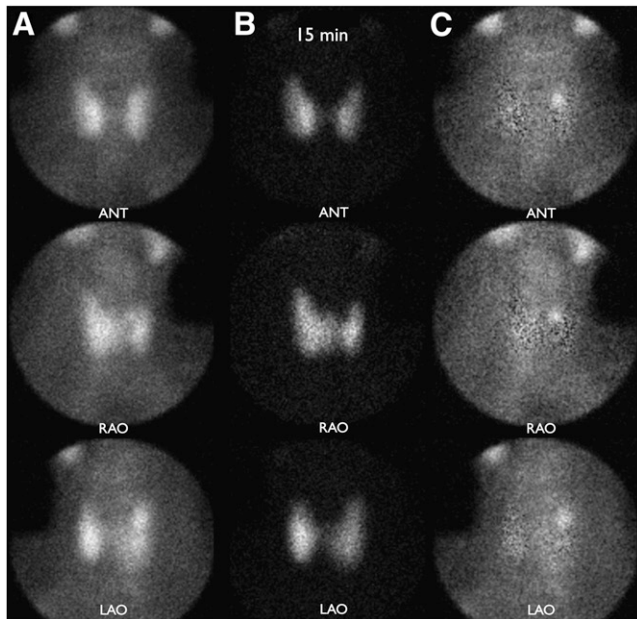
FIGURE 2. Example of double-tracer, single-phase protocol from same patient as shown in Figure 1. ^{123}I was given orally 2 h before intravenous administration of ^{99m}Tc-sestamibi. Simultaneous pinhole images of ^{99m}Tc-sestamibi and ^{123}I were acquired of neck in anterior (ANT), right anterior oblique (RAO), and left anterior oblique (LAO) projections at 15 min after administration of ^{99m}Tc-sestamibi. In addition, simultaneous parallel-hole image of ^{99m}Tc-sestamibi and ^{123}I from submandibular glands to left ventricle was obtained in anterior projection at 15 min (not shown). Parathyroid adenoma is clearly seen at upper pole of left lobe of thyroid in subtraction images.

A failed to detect any of the 4 nonprimary adenomas and reader B failed to detect 3 of the 4 nonprimary adenomas. For the dual-tracer, single-phase protocol, readers A and B failed to detect 1 and 2, respectively, of the 4 nonprimary adenomas. And for the dual-tracer, dual-phase protocol, both readers A and B failed to detect 3 of the 4 nonprimary adenomas.

The percentage localization success rate for both readers is given in Table 2. For the 2 observers combined, the localization success rate was 66% for the single-tracer, dual-phase protocol, 94% for the dual-tracer, single-phase protocol, and 90% for the dual-phase, dual-tracer protocol. Both dual-tracer protocols were significantly more accurate than the single-tracer protocol ($P < 0.01$), and there was no significant difference between the 2 dual-tracer protocols. The 2 mislocalizations that occurred in the single-tracer protocol are combined with the undetected adenomas for each protocol. Again, there is a higher localization success rate for each of the 2 dual-tracer protocols compared with the single-tracer protocol ($P < 0.001$) and no significant difference between the 2 dual-tracer protocols.

It is considered good practice to mention possible secondary adenomas in the interpretation of parathyroid imaging studies in case there are multiple adenomas (3). At the time of surgery, if the serum parathormone level does not decrease appropriately after removal of the first ade-

noma, the surgeon then has a guide to the location of a likely second adenoma. Both reader A and reader B had false-positive single additional adenoma localizations in 5 patients; for only 1 of the patients was the error the same for both readers.

Of the adenomas that lay posterior to the thyroid and were detected, all moved relative to the thyroid in the anterior and posterior oblique images in a manner consistent with a posterior location. That is, compared with the position of the adenoma relative to the thyroid in the anterior image, the adenoma moved to the right relative to the thyroid in the right anterior oblique image and to the left relative to the thyroid in the left anterior oblique image. No adenoma was found anterior to the thyroid. Two of the intrathyroidal adenomas moved with the thyroid, and 1 appeared to move as if it were relatively posterior.

Based on imaging and surgical findings, there were 9 adenomas that were located posterior to the inferior portion of the thyroid by surgery and imaging, but were actually mildly ectopic superior parathyroid glands. In these cases a normal inferior gland was identified at surgery in addition to the inferiorly located adenoma. There was no instance of an inferior parathyroid gland that was located posterior to the superior poles of the thyroid gland.

DISCUSSION

This study demonstrates the superiority of a dual-tracer protocol using the simultaneous acquisition of ^{99m}Tc-sestamibi and ^{123}I in comparison to the commonly used single-tracer protocol using ^{99m}Tc-sestamibi imaging at 2 time points, 15 min and 3 h, for the detection and localization of parathyroid adenomas. In addition, the dual-tracer protocol did not benefit from delayed imaging at 3 h. Thus, the significantly higher accuracy of the dual-tracer protocol with ^{99m}Tc-sestamibi and ^{123}I can be achieved with only 1 imaging session instead of 2, and with a decrease in overall procedure time. Although the number of patients in this study was relatively small, the statistical significance of the results is quite high.

In the dual-tracer protocol, the simultaneous acquisition of ^{99m}Tc-sestamibi and ^{123}I images is critical. For small structures such as parathyroid adenomas, perfect coregistration is required to create confidence in the interpretation of small areas of residual activity after the subtraction process. Dual-tracer protocols without simultaneous acquisition leave the possibility of a change in patient neck rotation and angulation between acquisitions of the images with each of the tracers. These types of motions are difficult to detect and to compensate for during manual coregistration and subtraction. Although manual coregistration can theoretically correct for translational motion of the patient between nonsimultaneous acquisitions, the process is subjective.

The use of pinhole collimation for maximum spatial resolution and accuracy is essential in parathyroid imaging (8,27). Although not evaluated in the present study, it is well known that in the case of small structures such as the thyroid
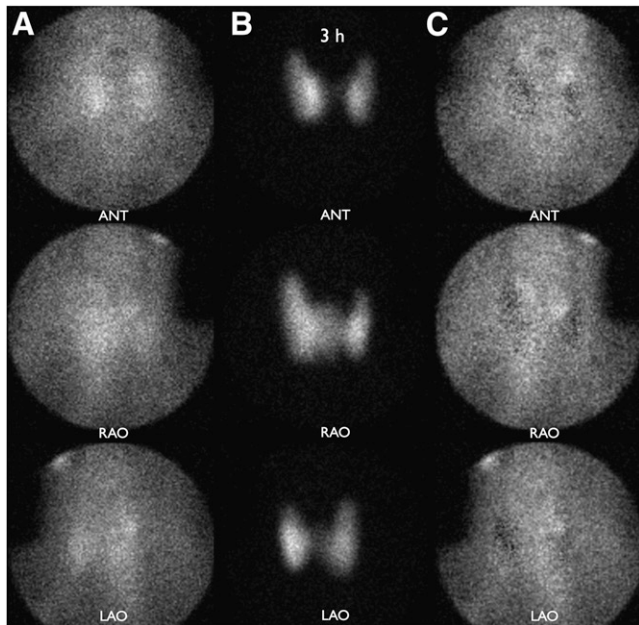
FIGURE 3. Example of double-tracer, double-phase protocol from same patient as shown in Figure 1. In addition to simultaneously acquired ^{99m}Tc-sestamibi and ^{123}I images at 15 min shown in Figure 2, same images were acquired again at 3 h. ^{99m}Tc-sestamibi washes out of parathyroid adenoma at same rate as it washes out of thyroid gland. ANT = anterior; RAO = right anterior oblique; LAO = left anterior oblique.

gland and parathyroid adenomas, pinhole collimation results in higher spatial resolution than parallel-hole collimation (3,8,27,28). Pinhole collimators can be placed at the optimal distance from the thyroid and parathyroid glands, but parallel-hole collimators must be kept some distance from the structures of interest to clear the face and chest in the anterior projection and the shoulders in the oblique projections.

The present study drew all 3 of the evaluated protocols from 1 parathyroid imaging study for each patient so that the evaluation of the 3 protocols was done on an intrapatient and intrastudy basis. This approach eliminates essentially all extraneous variables. In addition, no patient was eliminated because of previous parathyroid or thyroid surgery, and patients who were taking thyroid replacement hormone continued to do so during the imaging procedure.

The fundamental problem with the single-tracer, dual-phase protocol with ^{99m}Tc-sestamibi is that a significant number of parathyroid adenomas show washout of the tracer to the same extent as the thyroid gland (18,19). Therefore, any parathyroid adenoma that blends into the thyroid in early imaging and demonstrates washout of ^{99m}Tc-sestamibi in a fashion similar to the thyroid will go undetected or will be detected with reduced certainty in comparison to the dual-tracer protocol as used in this report.

There were 2 other findings of note in this study. One was that parathyroid adenomas that were at the same level as the thyroid all moved in the right and left anterior oblique images consistent with a location behind the thyroid except for 2 intrathyroidal adenomas that moved as if they were in the plane of the thyroid. Thus, parathyroid adenomas in an ectopic position anterior to the thyroid are unusual, and motion of a focus of activity consistent with an anterior location should suggest other etiologies such as a thyroid adenoma.

The second finding of note was that, of the 37 parathyroid adenomas that were not ectopic away from the thyroid, 9 were superior glands in an inferior position. Thus, when imaging shows a parathyroid adenoma behind an inferior pole of the thyroid gland, the location is likely to be correct but the gland may actually be a somewhat ectopic superior gland. In this case the surgeon is likely to find both the parathyroid adenoma and the normal inferior parathyroid gland in an inferior location. There was no instance of an embryologically inferior
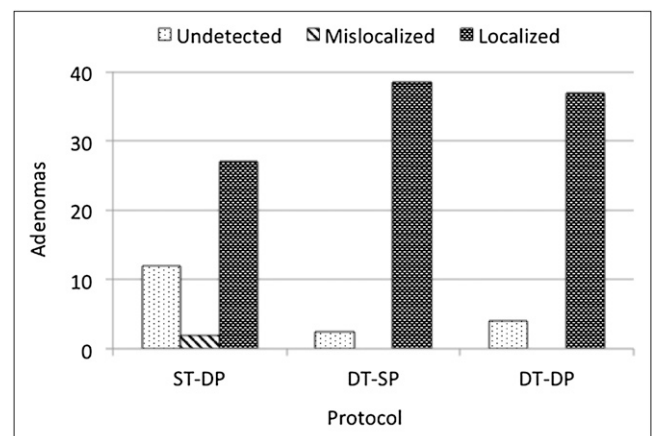
TABLE 1
Grading Results for Each of 3 Protocols for 41 Adenomas in 37 Patients

Protocol	Reader	Degree of certainty of location			
		0	1	2	3
ST-DP	A	17	7	11	6
	B	9	8 (1)	8 (1)	16
DT-SP	A	1	10	11	19
	B	4	11	5	21
DT-DP	A	3	10	9	19
	B	5	6	9	21

0 = no adenoma seen; 1 = possible adenoma; 2 = probable adenoma; 3 = definite adenoma; ST-DP = single-tracer, dual-phase; DT-SP = dual-tracer, single-phase; DT-DP = dual-tracer, dual-phase.

Numbers in parentheses indicate numbers of localizations that were incorrect.

FIGURE 4. Performance of each of 3 protocols is shown for correctly localizing position of 41 parathyroid adenomas in 37 patients. Data represent average results for 2 readers. ST-DP = single-tracer, dual-phase, DT-SP = dual-tracer, single-phase, DT-DP = dual-tracer, dual-phase.

TABLE 2
Localization Success for Each of 3 Protocols

| Protocol | Reader | Localization success | | |
		Adenomas	Correct	95% CI
ST-DP	A	24/41	59%	42–74
	B	30/41	73%	57–86
DT-SP	A	40/41	98%	87–100
	B	37/41	90%	77–97
DT-DP	A	38/41	92%	80–98
	B	36/41	88%	74–96

CI = exact binomial confidence interval; ST-DP = single-tracer, dual-phase; DT-SP = dual-tracer, single-phase; DT-DP = dual-tracer, dual-phase.

Calculations are on per-adenoma basis. There were 41 adenomas in 37 patients.

parathyroid gland that was located ectopically posterior to the superior pole of the thyroid gland.

Although the superior accuracy of simultaneous acquisition of ^{99m}Tc-sestamibi and ^{123}I with perfectly coregistered subtraction has been reported in the literature since the 1990s (4,14,15), the single-tracer, dual-phase ^{99m}Tc-sestamibi protocol is still commonly performed (20). The single-tracer, dual-phase ^{99m}Tc-setamibi protocol is the only protocol given in 2 standard nuclear medicine textbooks published in 2006 (15,16); is considered equal to the dual-tracer protocol in the 2004 Society of Nuclear Medicine Procedure Guideline for Parathyroid Scintigraphy (29); is the preferred protocol, with the dual-tracer protocol given as a secondary option in the 2009 edition of a widely used nuclear medicine procedure manual (14); and is described as an acceptable alternative in the 2009 EANM Parathyroid Guidelines (17).

In the past, ^{123}I was relatively expensive and not readily available. In addition, dual-tracer protocols are considered relatively complex and time-consuming. However, because the second phase of the dual-tracer protocol does not increase accuracy, a dual-tracer, single-phase protocol can be used. Elimination of the second imaging session offsets the additional cost of the second tracer, and the overall procedure time is less. The use of ^{123}I in addition to ^{99m}Tc-sestimibi adds a small amount of radiation to the study, but this small increase in diagnostic radiation is justified by the 43% increase in accuracy of localizing parathyroid adenomas in the dual-tracer, single-phase protocol compared with the single-tracer, dual-phase protocol.

The usefulness of SPECT and SPECT/CT was not evaluated in the present study. Dual-tracer (^{99m}Tc-sestamibi and ^{123}I), simultaneous acquisition with SPECT or SPECT/CT has the advantage of providing better 3-dimensional information and higher contrast than imaging with pinhole collimation in the anterior and anterior oblique projections (5,8,11,27). However, pinhole collimation has higher spatial resolution than the parallel-hole collimation images that are used to generate SPECT images (30). Anterior and an-

terior oblique pinhole imaging has been shown to be superior to SPECT without anterior oblique pinhole imaging (8). The lower spatial resolution of parallel-hole collimation can be eliminated by performing pinhole SPECT, but this capability is not widely available (31,32). Future direct comparison of planar pinhole imaging (as described in this report) with pinhole SPECT/CT, both with dual-tracer simultaneous acquisition, will be of interest.

CONCLUSION

This study demonstrated that parathyroid imaging with a protocol consisting of dual-tracer, single-phase simultaneous acquisition of ^{99m}Tc-sestamibi and ^{123}I with pinhole collimation has a high localization success rate of 94% and is significantly more accurate and results in a higher degree of diagnostic certainty than the commonly used single-tracer, dual-phase protocol with ^{99m}Tc-setamibi alone. In addition, the dual-tracer, single-phase protocol requires only 1 imaging session and reduces overall procedure time.

REFERENCES

1. Bringhurst FR, Demay MB, Kronenberg HM. Hormones and disorders of mineral metabolism. In: Kronenberg H, Melmed S, Polonsky K, et al. *Williams Textbook of Endocrinology.* 11th ed. Philadelphia, PA: Elsevier Saunders; 2008.
2. Doberry GM, Wells SA. Parathyroid glands. In: Townsend CM, Beauchamp R, Evers BM, Mattox KL. *Sabiston Textbook of Surgery: The Biological Basis of Modern Surgical Practice.* Philadelphia, PA: Elsevier Saunders; 2008.
3. Mullan BP. Nuclear medicine imaging of the parathyroid. *Otolaryngol Clin North Am.* 2004;37:909–939.
4. Neumann DR, Esselstyn CB, Go RT, et al. Comparison of double phase ^{99m}Tc-sestamibi with [123]I-^{99m}Tc-sestamibi subtraction SPECT in hyperparathyroidism. *AJR.* 1997;169:1671–1674.
5. Eslamy HK, Ziessman HA. Parathyroid scintigraphy in patients with primary hyper-parathyroidism: Tc-99m sestamibi SPECT and SPECT/CT. *Radiographics.* 2008;28:1461–1476.
6. Randall GJ, Zald PB, Cohen JI, Hamilton BE. Contrast enhanced MDCT characteristics of parathyroid adenomas. *AJR.* 2009;193:W139–W143.
7. Palestro CJ, Tomas MB, Tronco GG. Radionuclide imaging of the parathyroid glands. *Semin Nucl Med.* 2005;35:266–276.
8. Ho Shon IA, Yan W, Roach P, et al. Comparison of pinhole and SPECT Tc-99m-MIBI imaging in primary hyperparathyroidism. *Nucl Med Commun.* 2008;29:949–955.
9. Nichols KJ, Tomas MB, Tronco GG, et al. Preoperative parathyroid scintigraphic lesion localization: accuracy of various types of readings. *Radiology.* 2008;248:221–232.
10. Smith JR, Oates ME. Radionuclide imaging of the parathyroid glands: patterns, pearls and pitfalls. *Radiographics.* 2004;24:1101–1115.
11. Hindié E, Ugur O, Fuster D, et al. EANM Parathyroid Guidelines. *Eur J Nucl Med Mol Imaging.* 2009;36:1201–1216.
12. Ruda JM, Hollenbeck C, Stack BC. A systematic review of the diagnosis and treatment of primary hyperparathyroidism from 1995 to 2003. *Otolaryngol Head Neck Surg.* 2005;132:359–372.
13. Coakley AJ, Kettle AG, Wells C, et al. Tc-99m-sestamibi: a new agent for parathyroid imaging. *Nucl Med Commun.* 1989;10:791–794.
14. Klingensmith WC, Eshima D, Goddard J. Parathyroid imaging. In: *Nuclear Medicine Procedure Manual.* Englewood, CO: Wick Publishing; 2009.
15. Mettler FA, Guiberteau MJ. Parathyroid imaging. In: *Essentials of Nuclear Medicine Imaging.* Philadelphia, PA: Elsevier Saunders; 2006:96.
16. Ziessman HA, O'Malley JP, Thrall JH. Parathyroid scintigraphy. In: *Nuclear Medicine: The Requisites.* St. Louis, MO: Mosby; 2006:101.
17. 2009 EANM Parathyroid Guidelines. *Eur J Nucl Med Mol Imaging.* 2009;36:1201–1216.

18. Kulkarni KP, Van Nostrand D, Wells K, et al. The frequency of parathyroid adenomas and/or hyperplasia that have washout equal to normal thyroid tissue in patients who have a negative dual-time-point 99m-Tc sestamibi scan [abstract]. *J Nucl Med.* 2010;51 (suppl 2):56P.

19. Doumas A, Iakovou I, Boundas D, et al. How often are parathyroid adenomas expressing the same Tc-99m-sestamibi wash-out compared to adjacent thyroid parenchyma? [abstract]. *Eur J Nucl Med Mol Imaging.* 2009;36(suppl 2):716.

20. Tunninen V, Kauppinen T, Eskola H, et al. Variable imaging and processing protocols of parathyroid scintigraphy in Finland. *Eur J Nucl Med Mol Imaging.* 2009;36(suppl):S194–S233.

21. Hendie E, Melliere D, Jeanguillaume C, et al. Parathyroid imaging using simultaneous double-window recording of technetium-99m-sestamibi and iodine-123. *J Nucl Med.* 1998;39:1100–1105.

22. Arveschoug AK, Bertelsen H, Vammen B. Presurgical localization of abnormal parathyroid glands using a single injection of Tc-99m-sestamibi: comparison of high-resolution parallel-hole and pinhole collimators, and interobserver and intraobserver variation. *Clin Nucl Med.* 2002;27:249–254.

23. Hindié E, Melliere D, Jeanguillaume C, et al. Parathyroid imaging using simultaneous double window recording of technetium- 99m-sestamibi and iodine-123. *J Nucl Med.* 1998;39:1100–1105.

24. Jeanguillaume C, Urena P, Hindié E, et al. Secondary hyperparathyroidism: detection with I-123-Tc-99m-sestamibi subtraction scintigraphy versus US. *Radiology.* 1998;207:207–213.

25. Mettler FA, Bhargavan M, Thomadsen BR, et al. Nuclear medicine exposure in the United states, 2005-2007: preliminary results. *Semin Nucl Med.* 2008;38: 384–391.

26. Liang KY, Zeger SL. Longitudinal data analysis using generalized linear models. *Biometrika.* 1986;73:13–22.

27. Ho Shon IA, Bernard E, Roach P, et al. The value of oblique pinhole images in pre-operative localisation with ^{99m}Tc-MIBI for primary hyperparathyroidism. *Eur J Nucl Med.* 2001;28:736–742.

28. Heiba S, Rivera J, Jiang M, et al. The optimized evaluation of primary hyperparathyroid patients (PHP) with dual tracer (DT) neck pinhole (PH) and SPECT/CT imaging [abstract]. *J Nucl Med.* 2010;51(suppl 2):321P.

29. Greenspan BS, Brown ML, Dillehay GL, et al. The Society of Nuclear Medicine Procedure Guideline for Parathyroid Scintigraphy. Reston, VA: Society of Nuclear Medicine; 2004.

30. Levine DS, Belzberg AS, Wiseman SM. Hybrid SPECT/CT imaging for primary hyperparathyroidism. *Clin Nucl Med.* 2009;34:779–784.

31. Spanu A, Falchi A, Manca A, et al. The usefulness of neck pinhole SPECT as a complementary tool to planar scintigraphy in primary and secondary hyperparathyroidism. *J Nucl Med.* 2004;45:40–48.

32. Carlier T, Oudoux A, Mirallie E, et al. Tc-99m-MIBI pinhole SPECT in primary hyperparathyroidism: comparison with conventional SPECT, planar scintigraphy and ultrasonography. *Eur J Nucl Med Mol Imaging.* 2008;35: 637–643.